BioEnergy Research (2021) 14:991–1001
https://doi.org/10.1007/s12155-020-10200-0

Renewable Bio-Oil from Pyrolysis of *Synechocystis* and *Scenedesmus* Wild-Type Microalgae Biomass

Masoud Derakhshandeh[1] · Funda Ateş[2] · Umran Tezcan Un[3]

Received: 26 June 2020 / Accepted: 1 October 2020 / Published online: 6 October 2020

Abstract

In this study, biomasses of microalgae *Scenedesmus* and *Synechocystis* species were thermochemically converted to biofuel in a fast pyrolysis process. The effect of pyrolysis temperature on the products yield was investigated. The optimal pyrolysis temperature for *Scenedesmus* and *Synechocystis* biomass was 500 °C and 600 °C, respectively, resulting in higher bio-oil yield of 35.3 wt% and 21.1 wt%. The produced bio-oil had higher high heating value (HHV) (35–40 MJ/kg) than that of beech wood source bio-oil (23–35 MJ/kg). The obtained biochar had low surface area but with considerable nitrogen, phosphorus, and other mineral content was suggested as fertilizer. It was concluded that the microalgae type and its cultivation and harvesting method affects the characteristics of the products and final energy efficiency as well. Energy efficiency assessment showed that the technology needs to be improved substantially to reduce the energy demand in cultivation, harvest, and pyrolysis step to be energy efficient.

Keywords Microalgae · Biofuel · Energy assessment · Thermochemical conversion · Bio-oil

Introduction

The growing demand for energy and the increasing carbon dioxide emissions are challenging concerns of the world. Renewable energy while being carbon neutral resources have emerged as a remedy for these concerns [1–3]. Biofuels as a significant group of renewables are categorized into multiple generations based on the nature of raw material being used. The microalgae-based biofuels are among third-generation biofuels which do not rely on edible material and arable lands [1, 3]. Microalgae are interesting biomass producers because of their fast-growing characteristics [4]. They are also interesting for not competing with agriculture products as is unfortunately happening for crop-based biofuels. Autotrophic nature of microalgae growth made them promising technology for carbon dioxide mitigation. Microalgae-dried mass is composed of mainly lipid, carbohydrates, and proteins [5]. The lipid part can be used for oil-based biofuels like biodiesel while the carbohydrates are suitable for bioalchohol production. The lipid extraction from microalgae cells is a challenging task with many studies reporting development of new methods [6, 7]. Different biofuels have been produced from microalgae biomass either through thermochemical conversion methods like gasification, thermochemical liquefaction, and pyrolysis to produce syngas, charcoal, and bio-oil including bioethanol, biodiesel, or through biochemical conversion methods like anaerobic digestion, fermentation, and photobiological hydrogen production to produce mainly methane, ethanol, and hydrogen [8]. Pyrolysis is a thermal conversion through depolymerization of organic material in the absence of oxygen into bio-oil suitable to be used as fuel [9–12]. Pyrolysis unselectively converts the biomass to fuel, and products are mainly liquids and solid char, both being valuable as fuel. Generally, the liquid products are more favorable for ease of transportation and application. In fast pyrolysis, the process parameters can be adjusted so that the liquid product will be maximized [12–16]. The biochemical composition of feed

Electronic supplementary material The online version of this article (https://doi.org/10.1007/s12155-020-10200-0) contains supplementary material, which is available to authorized users.

✉ Masoud Derakhshandeh
mderakhshandeh@gelisim.edu.tr

[1] Engineering Faculty, Life Science and Biomedical Engineering Application and Research Center, Istanbul Gelisim University, 34310 Istanbul, Turkey

[2] Department of Chemical Engineering, Eskişehir Technical University, 26555 Eskisehir, Turkey

[3] Department of Environmental Engineering, Eskişehir Technical University, 26555 Eskisehir, Turkey

biomass is also a determining factor where higher fat content improves the conversion yield and final bio-oil product characteristics.

Fast pyrolysis which is known by very short residence time of 1 to 3 s and temperature of around 500–600 °C is reported to have high bio-oil efficiency for microalgae [14, 17]. Multiple species of microalgae have been investigated like strains of chlorella [11, 12, 17], *Scenedesmus* [18], *Dunaliella* [19], *Nannochloropsis* [20], and Spirulina [9, 21].

Miao et al. [14] has used a fluidized bed reactor to perform fast pyrolysis of Chlorella protothecoides and *Microcystis aeruginosa* where 18 and 24% yield was obtained for liquid products, respectively. In a separate study, they showed that metabolic controlling of the microalgae growth, i.e., using a heterotrophic rather than an autotrophic growth, can improve the yields significantly [17]. Use of catalyzer biomass like potassium fluoride on alumina [18], Ni/zeolite-Y [22], an TiO_2-supported Ni [23]in a catalytic pyrolysis of microalgae improved the yields and/or the products quality as was concluded by some researchers. Microwave-assisted pyrolysis was also reported to have better outcomes [19, 20].

There are few studies which report on the "cultivation to fuel" energy assessment of the whole process based on experimental data and the available studies use mimicked process data [24]. The presented studies rely on the simulation models like GREET (Greenhouse Gases, Regulated Emissions, and Energy use in Transport by Argonne National Lab. USA) [2] and SimaPro (by Life Cycle Strategies Pty Ltd., Australia) [25] or other similar methods [26] which based on the designed process scheme, the model calculates the energy efficiency, cost, and carbon dioxide emission.

In the present study, the characteristics of bio-oil produced from biomass of two different strains of microalgae have been investigated. Wild-type *Scenedesmus* and *Synechocystis* microalgae were isolated from local streams and used as biomass producers. The fast pyrolysis process at different temperatures was applied to obtain bio-oil. The characteristics of such products were investigated in detail. Finally, based on the observed rate of biomass production of microalgae and the obtained bio-oil yield, large-scale application of microalgae technology was evaluated compared with a fossil crude oil factory input capacity. The energy efficiency of the whole process from microalgae cultivation to bio-oil was evaluated as well.

Materials and Method

Chemicals

The chemicals $NaNO_3$, K_2HPO_4, $MgSO_4.7H_2O$, $CaCl_2.2H_2O$, Citric acid, ammonium ferric citrate, $EDTANa_2$, Na_2CO_3, H_3BO_3, $MnCl_2.4H_2O$, $ZnSO_4.7H_2O$, $Na_2MoO_4.2H_2O$, $CuSO_4.5H_2O$, and $Co(NO_3)_2.6H_2O$ were used during microalgae culturing and large volume cultivation, purchased from Sigma-Aldrich, USA. Acetone, chloroform, methanol, phenol, sulfuric acid, KCl, and propanol were provided by Tekkim, Turkey. All the chemicals were of reagent grade. Reagent water was utilized in laboratory using a water purification unit (Thermo Scientific, Germany). Dichloromethane (DCM) was used as solvent for pyrolysis liquid product provided by Sigma-Aldrich, USA. Sodium sulfate anhydrous was used to dehydrate the pyrolysis liquid product, also purchased from Sigma.

Microalgae Strain and Cultivation

The wild-type strains of *Scenedesmus* (SCE) and *Synechocystis* (SYN) microalgae were isolated from the Porsuk River (Eskisehir, Turkey, 39° 46′ 12.0″ N 30° 29′ 54.6″ E) as was described in our previous work [27]. The medium for cultivation was BG11 according to [28]. The isolated microalgae were then batch cultured by transferring to 250-ml flasks. After almost 3 weeks and clear growth, cultures were transferred to 1-l volume flasks used as photobioreactors. At this stage, the culture solution was bubbled with a continuous 0.1 vvm gas stream of 5% CO_2 mixture with air (MKS instruments, USA) and kept under 3500 lx (T-10MA Konica Minolta; Japan) white fluorescent light (15 w, ORSAM, Turkey). To produce enough biomass, larger photobioreactors were implemented. Based on previous experiences, for SCE sp., a bubble column type (Supplementary Data) and for SYN a rectangular cross section configuration (Supplementary Data) was used. SCE sp. had a large cell size and could settle easily when mixing was stopped; therefore, the bubble column was a good choice. On the other hand, the SYN sp. which was floating in the solution was very stable so that even with no mixing for long time, they still could stay floated. The mass production rate of SYN was low. Therefore, a rectangular type photobioreactor with 50-l volume was used. The growth condition was adjusted as described for 1-l flask step unless that the light was provided by white light LED strips (5 m per reactor, 15 W/m) twisted around the reactors so that 3500 lx light intensity was maintained. The well-grown cultures in 1-l flasks were transferred to the large photobioreactors and the adequate amount of BG11 solution was added. Samples were taken regularly to monitor the growth by reading the optical density (OD) at 680 nm (Shimadzu UV-1800 UV-Vis Spectrophotometer). The OD was converted to g/l in dried mass basis using conversion factors withdrawn for each species after calibration of OD vs. biomass concentration in dried basis (db). When the growth curve appeared to reach the stationary phase, the harvest was started by taking half of the solution. The reactors were then replenished with fresh BG11 medium and cultivation continued until sufficient amount of biomass was produced.

Biomass Harvest

Because of different settling characteristics of two species, two approaches were implemented for harvesting. Harvesting is actually a bottle neck confronting microalgae technology [29]. The SCE species could settle down easily so that the obtained sample was left for 24 h and the top clear layer was siphoned gently. Then, 2 l of deionized distilled water (DDW) was added to the residue and left overnight for settling. This was done to wash out the minerals in the medium left in biomass. Again, the top clear layer was siphoned and the residue was dried at 110 °C.

For the SYN, natural settling was not efficient; therefore, a chemical coagulation approach was implemented [27]. Aluminum sulfate as coagulant was added to the biomass solution so that the final concentration of aluminum sulfate was 0.4 g/l. The solution was mixed vigorously for 2 min and then with the clear appearance of the flocs mixer, speed was lowered and gentle mixing continued for 30 min. Then, the mixing was stopped and left overnight. The clear top layer was siphoned and the residue was washed with DDW as described before. The washing was repeated 2 or 3 times to ensure the abatement of residual aluminum sulfate. Finally, the biomass residue was dried at 110 °C.

Biomass Characterization

The elemental analysis was done using a CHN analyzer (FlashSmart, Thermo Fisher). A scanning electron microscope (SEM, TM3030, HITACHI) device in combination with an Energy Dispersive X-Ray Spectrometer (EDX) equipped with Silicon Drift Detector (SDD) was used to quantify O, Al, S, Cl, K, and P elements. For liquid products, O was estimated by difference.

The lipid content was gravimetrically determined according to Bligh and Dyer [30] using methanol/chloroform as solvents. The carbohydrate part was colorimetrically estimated at 490 nm (Shimadzu UV-1800 UV-Vis Spectrophotometer) using sulfuric acid/phenol approach according to Dubois et al. [31] with dextran as standard carbohydrate. The protein content was estimated from elemental nitrogen and a conversion factor of 4.78 ± 0.62 as was suggested in a previous study [32] for microalgae. Moisture, ash, volatile material, and fixed carbon were determined according to ASTM D7582. High heating value (HHV) was estimated using the following formula proposed by Meraz and friends [33]:

$$\mathrm{HHV}\left({}^{\mathrm{Mj}}/_{\mathrm{kg}}\right) = (1-\mathrm{H_2O}/100) \times -0.3708[\mathrm{C}]-1.1124[\mathrm{H}] + 0.1391[\mathrm{O}]-0.3178[\mathrm{N}]-0.1391[\mathrm{S}]\Big) \quad (1)$$

Pyrolysis Setup and Procedure

The reactor was a UniTerm (Turkey) pyrolysis unit which the reactor vessel was an 80-cm-long steel pipe with an inner diameter of 8 mm. This unit had a very sensitive PID temperature control loop with a heating power of 2 kW. The vessel is made of special material which at the same time serves as a DC electric heater. A schematic of the whole unit is provided as supplementary data. Per each run, 3.0 g of biomass was taken. Biomass was formerly ground to have < 1 mm particles. A small amount, ~ 0.65 g, of crimped steel fiber was used to maintain a fixed bed and inserted into the reactor column by means of a long steel rod. Then, the biomass was poured from the top and with the same rod pushed toward the bed without pressing hard. The set points for pyrolysis temperature, heating rate, and time of pyrolysis were adjusted. When all the joints and connections were fixed, N_2 as carrying inert gas was flown (1 l/min) for almost 3 min to ensure abatement of oxygen in the reactor before applying electricity. This flow rate also maintains a residence time of 1–0.6 s for hot gas products. A control unit automatically operated the process upon start. Pyrolysis temperatures of 400, 500, and 600 °C and retention time of 3 min was followed as was also reported in [9, 34, 35]. Two replicates were done per each experiment and standard errors (SE) calculated where applicable.

The pyrolysis unit upon completion of run was left to cool down to 50 °C, and then, after stopping N_2 current, the joints opened, and the liquid product which was a highly viscose sticky paste was washed with DCM and collected [36]. The obtained product in this way was dehydrated by dripping the solution over a funnel filled with anhydrous sodium sulfate. The dehydrated solution was collected in a pre-weighed evaporating flask. DCM was dripped over the funnel to ensure complete gain of product. The collected solution at the bottom was again concentrated by evaporation of DCM using rotary evaporator at 40 °C and 750 mmHg vacuum (Heidolph, Germany). Evaporation continued until no dripping was observed in condenser side. Then, the evaporating flask was detached and left under hood and regularly weighted till constant weight. The final weight was recorded for liquid product yield calculation (Eq. 2). The obtained liquid product was then transferred with the help of some droplets of DCM to glass containers and the containers cap were left half closed to let the excess DCM evaporate. After some days, the cap was tightened and the product stored in 4 °C. The solid part of the product along with the steel fiber bed was taken out of the column with the help of a long steel rod and weighted. This value was used for produced char yield calculation (Eq. 3). The char was stored in a tight cap falcon for later analysis. The gas yield was calculated by difference (Eq. 4).

$$\text{BioOil yield}\ (\%) = \frac{\text{biooil (gr)}}{\text{biomass (gr)}} \times 100 \quad (2)$$

$$\text{Char yield } (\%) = \frac{\text{char (gr)}}{\text{biomass (gr)}} \times 100 \quad (3)$$

$$\text{Gas yield } (\%) = 100 - \text{bioOil}(\%) - \text{char}(\%) \quad (4)$$

Analyses of Product

The liquid and solid products were analyzed for elemental CHN and oxygen content was calculated by difference [35]. Then, FTIR analysis (Nicolet iS10, Thermo Scientific) was performed to determine the functional groups [11, 35]. Liquid products were subjected to GS-MS analyze to find out the constituents [11, 23, 36].

Surface area of the biochar was estimated using Brunauer-Emmet-Teller analyzer (BET, NOVAtouch, Quantachrome, UK) [11, 35, 37]. Degasification was performed before analysis at 450 °C under 38 Torr vacuum for 16 h. Topography of the biochar surface was evaluated using scanning electron microscopy (SEM, TM3030, HITACHI) [11, 35].

Energy Efficiency Assessment

The bio-oil energy flow was assessed using current study's experimental data, thermodynamic calculations, and published literature data with some assumptions. Estimations were done for the real case of this study. The operational energy need of PBRs is calculated according to the process parameters. The harvesting energy included the mixing energy during flocculation and thermal drying. The pyrolysis energy was calculated using thermodynamic and heat transfer relations [25].

$$Q_{req} = Q_{cul} + Q_{har} + Q_{pyr} \quad (5)$$

where Q_{req} is the required total energy (MJ), Q_{cul} is the cultivation energy demand, Q_{har} is harvesting energy demand, and Q_{pyr} is the pyrolysis energy demand. Cultivation energy goes for (a) gas supply line to compress the air/CO_2 mixture so that overcomes the static pressure of the PBR, (b) light source, and (c) water and substrate charge into PBR.

Harvesting energy includes mixing during flocculation (where applied) and thermal drying.

Consumed energy was calculated using heating capacity of the reactor which was 2 kW.

The obtainable energy from the products is the embedded energy in the bio-oil and char.

$$Q_{gain} = Q_{bioOil} + Q_{char} \quad (6)$$

The embedded energy in the bio-oil and char was estimated using HHV correlations as in [4, 38].

Results and Discussion

Microalgae Cultivation

SCE sp. had a green color while SYN sp. looks blue-green which is the characteristics of their belonging microalgae families chlorophyte and cyanophyte, respectively. The obvious larger size of the SCE sp. is an advantage during harvest because they settle easily when mixing is stopped but is also a disadvantage during cultivation because continuous mixing is required to maintain homogeneous growth condition. The reverse applies for SYN. The growth curves are presented in Fig. 1. The SCE growth in bubble column reactor had better performance than the SYN in rectangular cross section reactor perhaps because of more efficient mixing. At the linear region, SCE growth rate was 80 mg/l.d whereas this value for SYN was 17 mg/l.d.

Biomass Characteristics

SYN sp. compared with SCE sp. had much smaller cell size being approximately 3–4 μm against 20–30 μm for SCE. The smaller cell size in practice could result in a denser dried biomass, something that was revealed in SEM image of dried biomass (Supplementary data). There are other factors which also affect the mechanical property of biomass like method of harvest. In the SEM images of dried biomass, the cells are not distinguishable because of the deformations and mild sintering of the cells and liquid extracts during drying step. It seems that very small pores are also formed during drying, perhaps because of moist evaporation. The structure of SCE biomass seems to be more porous than SYN biomass which was related to the application of coagulant during harvest of SYN and also cell morphology as well. Porous structure helps more uniform and efficient heat transfer by convectional

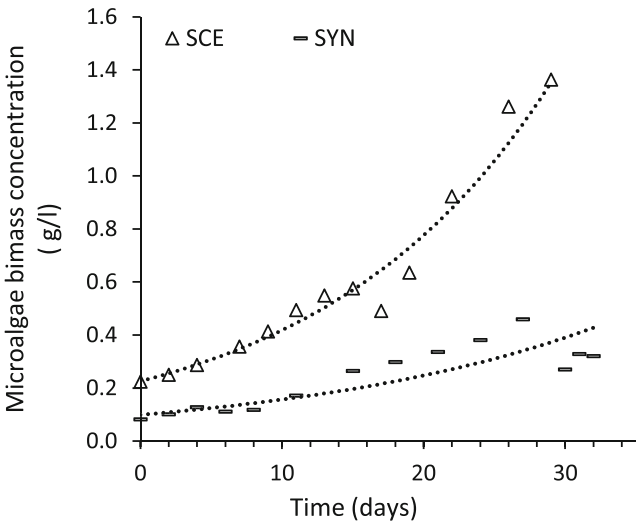

Fig. 1 Growth curve of microalgae species

circulation of hot gases. The organic nature of biomass hinders efficient heat transfer. The proximate analysis, ultimate analysis of CHN/O in dried basis wt% (db) and dried ash free basis wt% (daf), and elemental and biochemical composition of the biomasses are summarized in Table 1. For comparison, the data for wood is also included in Table 1 which is taken from the published work of Trinh and friends [1]. The volatiles for SCE and SYN were 85.3 and 73.7 wt% db. This value for wood was 84.3 wt% db [1]. Analyses of biochemical composition showed that biomass was mainly composed of lipid, protein and carbohydrate which for SCE were 47.3, 43.2, and 41.0 wt% whereas for SYN were 4.2, 52.8, and 26.6 wt%, respectively. Lipid and carbohydrate content of SCE was higher than for SYN where on the contrary, the protein content of SYN was higher. The ash residue of SYN (15.2 wt%) was much higher than SCE (2.7 wt%) due to the different way of harvest since SCE was left to settle without addition of coagulant but for SYN was used. The elemental aluminum in the biomass for SYN represented 4.41 wt% db of the biomass. Aluminum sulfate was used during coagulation, precipitated as $Al(OH)_3$, and caused floc formation. Low ash is advantageous from an application point of view especially when the energy of the biomass is going to be directly extracted through combustion. Accumulation of high ash in burners especially with obstacles confronting conveying solid material shall be avoided.

This was observed that the oxygen content of SYN biomass was 38.8 wt% daf while for SCE composed only 24.1 wt% daf but still lower than lignocellulosic resources [1]. The presented value for elemental CHN/O shows significant higher carbon content of SCE which was 62.1 wt% daf compared with 42.4 wt% daf for SYN. Higher carbon content results in higher HHV of SCE (30.90 MJ/kg) compared with SYN (22.6 MJ/kg). The high N content equal to 9.0 wt% daf for SCE and 11.0 wt% daf for SYN was a disadvantage of both microalgae biomass. In contrast, S content was insignificant. The N and S oxidize to NO_x and SO_x gases upon combustion.

Table 1 Proximate, ultimate, elemental, and biochemical analysis of microalgae biomass

	SCE	SYN	Wood[b]
Proximate analysis (wt%)			
Moisture	7.04 ± 0.33	9.56 ± 0.38	9.1
Ash (wt% db)	2.68 ± 0.09	15.12 ± 0.50	2.7
Volatile material (wt% db)	85.23 ± 0.07	73.65 ± 0.27	84.3
Fixed carbon (wt% db)	5.05 ± 0.17	1.67 ± 0.15	13
Ultimate analysis (wt% db)			
C	61.93 ± 1.67	39.70 ± 1.07	51.3
H	7.41 ± 0.07	7.3 ± 0.07	5.7
N	9.01 ± 0.24	10.34 ± 0.28	0.21
O[a]	24.13 ± 0.51	36.32 ± 0.86	40.5
Ultimate analysis (wt% daf)			
C	62.12 ± 1.66	42.39 ± 1.14	52.7
H	7.44 ± 0.07	7.8 ± 0.07	5.9
N	9.27 ± 0.25	11.04 ± 0.30	0.22
O	24.18 ± 0.52	38.78 ± 0.92	41.0
Elemental analysis[a] (wt% db)			
Al	0.34 ± 0.26	4.41 ± 1.15	0.05
S	0.65 ± 0.76	0.35 ± 0.22	0.03
Cl	na	0.11 ± 0.76	< 0.01
K	1.14 ± 0.93	0.84 ± 0.60	0.14
P	0.42 ± 0.18	1.66 ± 0.47	0.01
Biochemical composition (not normalized)			
Lipid	47.3 ± 0.4	4.23 ± 1.2	
Protein	43.2 ± 6.1	52.8 ± 7.2	
Carbohydrate	41.0 ± 2.6	26.6 ± 0.7	
HHV (MJ/kg)	30.9	22.6	

[a] Estimated by EDX

[b] Data for wood are taken from reference [1]

Pyrolysis Product Yield

The pyrolysis converted the biomass into solid, liquid, and gas products with different yields based on type of the microalgae and the temperature as is presented in Fig. 2. The highest liquid product yield for SCE was 35.3% obtained when the SCE biomass pyrolyzed at 500 °C, whereas for SYN, the largest yield 21.1% was obtained at 600 °C. For both biomasses, the lowest amount was produced at 400 °C with yields of 27.1 and 14.6%, respectively, for SCE and SYN. Greenhalf and friends [39] reported a bio-oil yield of 34.97% and 63.17%, respectively, from wheat straw and beech wood when subjected to pyrolysis at 520 °C. In another research [17], a bio-oil yield of 57.9% was reported for *Chlorella* microalgae biomass at an operating temperature equal to 500 °C. Generally, a higher yield was achieved from lipid-rich microalgae biomass than lignocellulosic biomass like [17]. Microalgae being a prokaryote microorganism owe a much simpler structure than eukaryotic plants with rigid cell walls that are interconnected firmly with long chains of polymerized lignin and cellulose. The main components of microalgae are lipid, carbohydrate, and proteins, whereas for higher plants, cellulose (~ 39%), lignin (~ 24%), and hemicellulose (~ 22%) compose almost more than 80% of the mass. Microalgae biochemical constituent is an important factor affecting bio-oil yield where higher lipid content is believed to enhance the bio-oil yield. Vardon et al. [16] showed that pyrolysis of a defatted *Scenedesmus* biomass resulted in 7 wt% decrease in yield compared with normal *Scenedesmus* biomass. This was also observed in this study where SYN biomass with 4.2 wt% lipid at the best case converted to 21.1 wt%

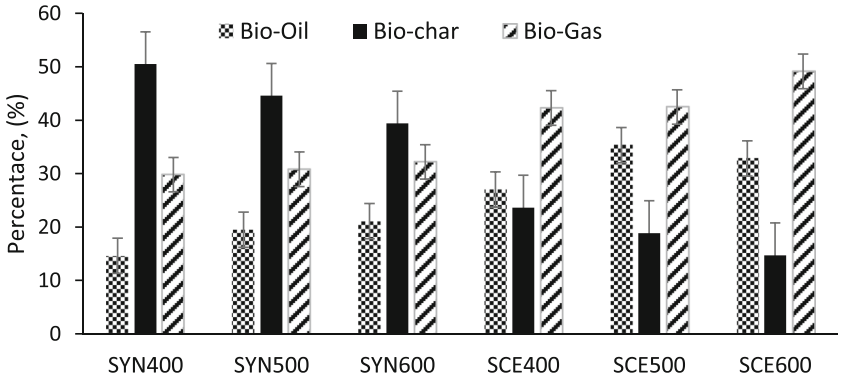

Fig. 2 The production yield of bio-oil, biochar, and biogas for SCE and SYN biomasses at 400, 500, and 600 °C

bio-oil, and SCE biomass with 47.3 wt% lipid gave 35.3 wt% bio-oil yield.

At the pyrolysis temperature where maximum liquid was produced, the biochar was minimized comparing to the other temperatures. It was also observed that the increase of temperature increased the gas product yield for both biomass although this was less significant for SYN. For SYN, the obtained biochar yields at 400 °C and 600 °C were 50.5 and 39.4%, respectively. For SCE samples, this was 23.6 and 14.7% accordingly. It was clear that the lower pyrolysis temperatures enhanced solid products or biochar yield. In general, biochar composed higher proportion of products for SYN comparing to SCE. Low pyrolysis temperature favors biochar production because of uncompleted decomposition of biomass. Therefore, lower pyrolytic conversion at reduced temperatures resulted in high char yield and low oil product yield.

Biogas was calculated by difference. The highest biogas proportion was observed at 600 °C for SYN and SCE, respectively, being 32.2 and 49.1%, respectively. The significant higher biogas and also liquid product yield for SCE comparing to SYN were related to the higher lipid content of SCE biomass because small chain fatty acid evaporate or decompose to gas products more readily. In addition, the more porous structure of SCE compared with SYN (Supplementary data) facilitates uniform high temperature in the center of biomass particles by hot convections.

In general, the results in Fig. 2 showed that the pyrolysis yield was strongly dependent on the temperature which indicates, for a large-scale application, careful control of the temperature, and maintaining homogeneous temperature profile in the reactor has crucial importance.

Bio-Oil Characteristics

Bio-oil produced from microalgae in appearance was a dark brownish sticky paste with low mobility in room temperature (~20 °C). It was important to be addressed because the liquid nature of the bio-oil is always magnified for transportation capability through pipelines. For such a goal, bio-oil in this form may need heating or addition of solvents at dispatch and re-evaporating at receiving point or application of cracking techniques for conversion of bio-oil to even lighter compounds to make the pumping task economically feasible.

The CHN/O analyses of the bio-oil products are presented in Table 2. These data reveals that comparing to the original biomass, the liquid product had less nitrogen content. For SCE, it was 8.00, 6.92, and 7.62 wt%, respectively, for pyrolysis temperatures of 400, 500, and 600 °C. This value for SYN bio-oil was 9.95, 9.46, and 9.50 wt% accordingly with no considerable variation at different temperatures. For both species, the lowest nitrogen belonged to the temperature where highest bio-oil efficiency was achieved. This can be related to the favorable effect of lipid content on the quality of bio-oil where higher lipid content as for example in SCE samples corresponds to lower protein content of that samples and consequently lower nitrogen content in the liquid product. For bio-oil quality, low nitrogen and sulfur are interested for reduced pollution upon combustion. Trinh et al. [1] has reported 0.5% and 1.62% nitrogen in bio-oil of wood and straw, respectively. Clearly, nitrogen content of microalgae bio-oil as in the present study was much higher which was related to the fact that microalgae have high protein content compared with wood.

The oxygen content for SCE bio-oil was 10.87, 16.45, and 12.86 wt% whereas for SYN bio-oil was 9.23, 9.11, and 15.97 wt%, respectively, at 400, 500, and 600 °C. The increase in the oxygen content of bio-oil at higher pyrolysis temperatures was also reported elsewhere [22] and could be related to the lower share of aliphatic hydrocarbons at higher temperatures which is in contrast more favorable for production of polycyclic aromatic hydrocarbons and oxygenated compounds which have a higher oxygen content. The presence of oxygenated compounds at higher temperatures was also confirmed by the GC-MS analysis results which are presented as supplementary data. In previous studies, oxygen content of bio-oil was reported 19.43 wt% for chlorella microalgae [14], 35.3 wt% for wood oil, and 31.3 wt% for straw oil [1]. It was observed that the oxygen was less in microalgae bio-oil comparing to lignocellulosic bio-oil, something that was also considered by Wang and friends [12].

Table 2 Elemental analysis and HHV values for bio-oils

	C (wt%)	H (wt%)	N (wt%)	O (wt%)	O/C	HHV (MJ/kg)
SYN400	72.06 ± 1.96	8.76 ± 0.23	9.95 ± 0.29	9.23 ± 0.22	0.13	38.45
SYN500	71.33 ± 2.04	10.12 ± 0.93	9.46 ± 0.53	9.11 ± 0.26	0.13	39.54
SYN600	65.59 ± 1.78	8.94 ± 0.18	9.50 ± 0.31	15.97 ± 0.38	0.24	35.17
SCE400	71.11 ± 0.93	10.12 ± 0.11	8.00 ± 0.73	10.78 ± 0.15	0.15	38.78
SCE500	67.17 ± 1.10	9.48 ± 0.52	6.92 ± 0.09	16.45 ± 0.38	0.24	35.47
SCE600	70.08 ± 1.16	9.44 ± 0.81	7.62 ± 0.44	12.86 ± 0.30	0.18	37.23

Lower oxygen is beneficial for stability of the product and also higher HHV value [17] since presence of oxygen represents high concentration of organic compounds with oxygenous functional group like phenol and its derivatives which are unstable products [37]. The calculated HHV value (Table 2) for produced bio-oil samples was in the range 35–40 MJ/kg which was higher than HHV of SCE biomass (34.29 MJ/kg) and significantly higher than SYN biomass (19.49 MJ/kg). For lignocellulosic origin bio-oil, HHV in the range 23–35 MJ/kg was previously reported [1, 36]. The significant increase of HHV originates from both higher carbon and lower oxygen content of microalgae bio-oil comparing to wood biomass. This is because up to 70% of the non-condensable gas [12] in pyrolysis consist of CO_2 which means O/C proportion in the bio-oil improves during pyrolysis.

FTIR Spectroscopy

The FTIR chromatogram of the bio-oil is presented in supplementary figure (Supplementary data figure S.1–6) in the appendix. The wide peaks on the spectrum along with the high absorbance for most of wavenumbers revealed that a very complex mixture with variety of functional groups were present in samples. The similar spectrum of all six bio-oil samples revealed their similar chemical composition with some concentration variations. The peaks on the spectrum mainly correspond to aromatics, carboxylic acids, hydrocarbons, and amine compounds. Unless for the range of 1900–2500 cm^{-1} and > 3500 cm^{-1} there was strong absorbance on the rest of the spectrum. Very low absorbance at 2000–2500 cm^{-1} range reveals the absence of nitrile compounds. The spectra were interpreted with reference to previous similar studies [16, 34, 40]. The high absorption spectra in the range 3200 and 3550 cm^{-1} are assigned to either O–H (H-bonded) as in phenolic compounds or N–H stretching bonds representing hydroxyl or amine group compounds in the bio crude. Very strong absorption corresponding to CH_3, CH_2, and CH stretch (2840–3000 cm^{-1}) and their medium intensity bending vibrations (respectively, 1350–1470 cm^{-1}, 1370–1390 cm^{-1}, and 720–725 cm^{-1}) were observed. Additionally, peaks corresponding to heteroatom-containing functional groups appeared in all samples (1800–600 cm^{-1}). Peaks at ~ 1709 cm^{-1} were possibly due to H-bonded C=O group in carboxylic acids. Peak at around ~ 737 cm^{-1} and ~ 702 cm^{-1} could be due to =C–H or C–H out of plane bending. Peak at ~ 1266 cm^{-1} was related to the C–N absorptions which are as in aromatic amines which appear in 1200 to 1350 cm^{-1} range.

GC-MS Analysis

The GC/MS technique was used to identify the components of the bio-oil samples and also quantify it by calculating chromatogram peaks area. The chromatograms are presented in supplementary figure S.7–12 in the appendix. As can be seen, the number of peaks is low which shows that the bio-oil from microalgae is less complex than the other lignocellulosic bio-oil. For example, in the work of Ateş and Işıkdağ [36], chromatogram of bio-oil from wheat straw showed almost 56 significant peaks. The less complex nature of microalgae bio-oil was related to the lack of lignocellulosic material in microalgae biomass [12]. The share of aromatics was low because they are mainly lignin-originated compounds [41]. Variety of organic groups including phenols, furfurals, terpene, carboxylic acids, nitriles, and aromatics were detected. Heptadecane, neophytadiene, 2-hexadecene, 3,7,11,15-tetramethy, (E)-6,6-dimethylcyclooct-4-en-1-on, pentadecanenitrile, 2-hydroxy-3,5,5-trimethyl-2-cyclohexenone, n-hexadecanoic acid, phytol, 9-octadecenoic acid, and hexadecanamide were the most common compounds ranging from 1.5 to 35.06 wt% of the bio-oil composition. Interestingly, nitrogen-containing compounds were found more frequently in SYN biomass which was related to higher protein content of SYN species. It was concluded that the SCE biomass which had higher lipid content provided higher quality products as biofuel. This was also suggested elsewhere [17]. Phytol, an acyclic diterpene alcohol which originates from lipid, was more abundant in SCE bio-oil. Phytol is also a valuable chemical used as precursor for commercial synthesize of vitamins [42]. Neophytadiene which is a terpenoid, along with n-hexadecanoic acid and 9-octadecenoic acid, was other abundant lipid-derived compounds. Significant amount of heptadecane, an alkane hydrocarbon, was detected in SYN bio-oil which was advantageous for biofuel quality. In general, more volatile and light organics

were contained in SYN bio-oil compared with SCEN bio-oil. It could be related to the catalytic role of Al present in the biomass. The catalytic role of Al was investigated elsewhere [43]. It was also observed that for SCE, the composition did not change with temperature significantly, but for the SYN samples, the bio oil composition shifted toward lighter and/or smaller compositions which had less retention time with the increase of temperature which can be related to chain cracking reactions at higher temperatures. Similar observations confirming the higher share of phenolic and aromatic derivatives were also reported in [44, 45]. The observed effectivity of temperature on the SYN species can be also related to the presence of Al and its catalytic effect in the dried biomass which was used during harvesting step (Table 1).

Biochar Characteristics

The SEM images of the biochar products as well as feed biomass at different temperatures are presented as supplementary data. The SEM images of the biochar products reveal that higher temperatures produce a more porous structure but still very less porous when compared with lignocellulosic feed stocks [46].

The results for surface area determination using BET analysis (Table 3) reveal very low porosity of the microalgae biochar. While for some of the samples, the value was not in detectable range of the device, the obtained highest value was 4.85 m^2/g for SYN biomass at 500 °C and 6.1 m^2/g for SCE at 600 °C. In a previous study, 175.4 m^2/g was reported for biochar obtained from pitch pine [35].

CHN/O elemental analysis of biochar and also inorganic mineral contents is summarized in Table 3. Carbon element proportion decreases with the increase of temperature for both species. Carbon composed about 70.2 wt% of the SCE biochar and 53.8 wt% of the SYN biochar produced at 400 °C. Lower carbon of the SYN biochar was because of high amount of inorganic element and especially Al which was added during harvest as coagulant something that was not detected in SCE biochar.

Nitrogen has decreased in biochar for both biomasses compared with initial feed stocks, but still, nitrogen composed a considerable proportion in the range of 3.06–8.42 wt% for SYN and 3.4–7.5 wt% for SCE. Nitrogen along with other soil nutrients like P, K, and Mg suggests potential use of biochar as fertilizer.

Energy Efficiency Assessment

Energy efficiency assessment for bio-oil and char production together helps us to have better judgment about the feasibility of the whole process. The consumed energy in each step was calculated or measured using mentioned methods as in supplementary data file. The production of dried biomass in bubble column reactor (BC) needed 8.26 MJ/g biomass, whereas in rectangular (REC) type, 20.82 MJ/g was estimated. The cultivation energy is presented in Fig. 3. For both reactors, the most energy-intensive part was the light energy with 6.26 and 13.82 MJ/g, respectively, for BC and REC. The light energy can be excluded in real large-scale application using solar light. The energy required for continuous aeration was 1.99 and 6.98 MJ/g of biomass, respectively, for BC and REC reactors.

Input-consumed energy in cultivation, harvest, and pyrolysis steps for BC reactor was, respectively, 8.26, 0.05, and 0.12 MJ per gram of produced or transformed biomass (Table 4). Similarly, for REC reactor, these values were 20.82, 0.06, and 0.12 MJ. These are also presented in Table 4. It is clear that the most energy-intensive part was the cultivation step. The cultivation energy was responsible for almost 99% of total energy for both reactors.

The ratio of obtainable energy from pyrolysis products including bio-oil and char to the total consumed energy reveals weather the process was efficient or not. The obtainable energy is estimated using embedded energy as HHV for bio-oil and char as provided in Tables 2 and 3. The average values were then 37.44 and 22.23 kJ per gram of bio-oil and char, respectively. Among the tested cases, SCE500 had the highest bio-oil yield of 35.35 and biochar of 18.85%. Therefore, per

Table 3 Elemental analysis of SYN and SCE biochars at 400, 500 and 600 °C

	C	H	N	O	Al*	BET (m^2/g)	HHV (KJ/g)
CHN analyze (wt%)							
SYN400	53.82 ± 0.83	3.21 ± 0.09	8.42 ± 0.22	34.55 ± 0.73	7.19 ± 1.55	1.84	21.44
SYN500	46.45 ± 0.13	3.97 ± 0.10	7.17 ± 0.04	27.59 ± 0.15	8.24 ± 2.20	6.1	20.13
SYN600	48.58 ± 0.66	2.93 ± 0.31	6.21 ± 0.37	21.36 ± 0.93	10.2 ± 0.44	n.d**	20.31
SCE400	60.38 ± 0.49	6.31 ± 0.51	7.50 ± 0.69	25.81 ± 1.15	0.59 ± 0.87	n.d	28.28
SCE500	45.39 ± 1.010	2.44 ± 0.14	4.72 ± 0.11	47.45 ± 2.05	n.d	0.01	14.48
SCE600	43.19 ± 0.85	1.76 ± 0.08	3.06 ± 0.40	51.99 ± 1.63	n.d	4.85	11.75

*Estimated by EDX

**Not detected

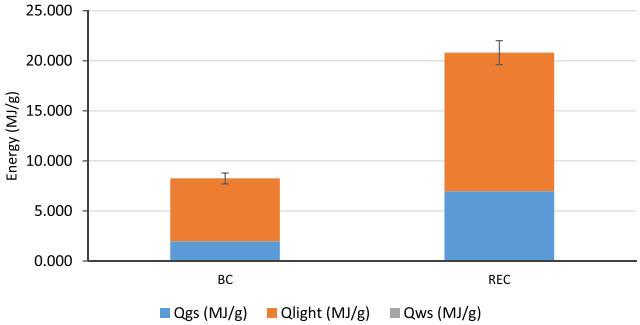

Fig. 3 Cultivation energy estimation for bubble column (BC) and rectangular (REC) type reactors

each gram of biomass as feed, 0.35 g bio-oil and 0.19 g of char would be obtained. These count for 17.30 kJ obtainable energy per each gram of pyrolyzed dried biomass. It is very much clear that the obtainable energy cannot compensate even the required energy for pyrolysis which needed 120 kJ/g. With the inclusion of biogas energy, the maximum obtainable energy would equal the embedded energy of fed biomass which was 30.9 kJ/g for the highest case. It was concluded that the whole processes need essential developments to obtain an energy efficient fuel.

Regarding cultivation step, light energy is naturally excluded because in a real case, the solar light is used. The other energy intensive part is the air compression which for a bubble column cannot be avoided, but using other reactors types like ponds and film reactors, this will be omitted. For open ponds, a mechanical mixing is used which consumes much less energy.

Many life cycle assessment studies are available reporting on the energy efficiency of microalgae to pyrolysis product which all of them concluded that the process was extremely inefficient [2, 25, 47], despite the fact that majority of these works are based on small-scale lab models and analogy with other available technologies. They still extremely suffer from optimism in their assumptions from different process energy consumption.

Bio-Oil Production in Large Scale

The result as was discussed above showed that pyrolysis of microalgae biomass provides a bio crude oil with high energy density. The HHV of the produced bio crude was almost 35 MJ/kg of biomass. It was comparable to that of fossil crude oil with HHV of 42–44 MJ/kg [48]. A large capacity fossil crude oil refinery facility like Ras Tanura Refinery (Aramco, Saudi Arabiya) can receive 550,000 bpd which roughly equals to 77,000 tons per day [49]. A photobioreactor facility which supposedly can produce enough biomass for bio crude oil feed of such refinery should have a volume of 1.2 billion m^3. Assuming that with the help of vertical photobioreactors, 1 m^3 volume would occupy just 1 m^2 of area, then the assumed photobioreactor facility will occupy 1200 km^2. This equals to the area of a 35-km-length square. As for now, this may seems far beyond practice, but one should consider the fact that this estimation was based on non-optimized growth condition. With efficient designs of vertical photobioreactors so that less area would be occupied (assuming 2 m^3/m^2) and also with optimization of microalgae growth rate for tenfold increase, the estimated required land area reduces by 20 times.

Altogether, a fast-growing nature of microalgae, high yield of bio-oil production, and the quality of such fuels make microalgae technology a promising solution for future energy demands.

Table 4 Energy requirements of different steps for both species

	Cultivation (MJ/g)	Harvest (MJ/g)	Pyrolysis (MJ/g)
SYN	8.262	0.049	0.120
SCE	20.825	0.058	0.120

Conclusion

Microalgae, a promising biomass feed stock, are known for their high biomass production rate and photosynthetic efficiency which are composed of mainly lipid, protein, and carbohydrate that can easily be converted thermochemically to liquid and solid biofuels which are believed to be advantageous over other lignocellulosic plant biomasses. As was observed in the present study, biomass could be efficiently converted to bio-oil with significant yield as high as 35.3 wt%. The high lipid content *Scenedesmus* species resulted in higher efficiency compared with *Synechocystis* species. The higher nitrogen content of the final products compared with that of wood sourced biomasses was a disadvantage, but in the contrary, their lower O/C ratio provides a more stable fuel with higher calorific value. Future attempts for increasing the rate of mass production and design of highly efficient photobioreactors are needed to make the microalgae technology feasible for large-scale application and especially biofuel plans. It was revealed that the obtainable energy from bio-oil cannot compensate even the required energy for pyrolysis which needed 120 kJ/g. This means pyrolysis of microalgae biomass has yet to be practically applicable. These improvements would focus on the cultivation step and harvesting where dewatering is the major energy demanding process.

Acknowledgments We thank "Plants, Drugs and Scientific Research Center of Anadolu university" (Anadolu Üniversitesi Bitki, İlaç ve Bilimsel Araştırmalar Merkezi, AÜBİBAM) for their support regarding analyses.

Funding This project was funded by the Anadolu University through research project no. 1702F050.

Data Availability All of the obtained data are provided in the manuscript.

Compliance with Ethical Standards

Conflict of Interest The authors declare that they have no conflicts of interest.

Code Availability Not applicable.

References

1. Trinh TN, Jensen PA, Dam-Johansen K, Knudsen NO, Sørensen HR, Hvilsted S (2013) Comparison of lignin, macroalgae, wood, and straw fast pyrolysis. Energy Fuel 27(3):1399–1409. https://doi.org/10.1021/ef301927y
2. Bennion EP, Ginosar DM, Moses J, Agblevor F, Quinn JC (2015) Lifecycle assessment of microalgae to biofuel: comparison of thermochemical processing pathways. Appl Energy 154:1062–1071. https://doi.org/10.1016/j.apenergy.2014.12.009
3. Lee RA, Lavoie J-M (2013) From first- to third-generation biofuels: challenges of producing a commodity from a biomass of increasing complexity. Anim Front 3(2):6–11. https://doi.org/10.2527/af.2013-0010
4. Derakhshandeh M, Tezcan Un U (2019) Optimization of microalgae Scenedesmus SP. growth rate using a central composite design statistical approach. Biomass Bioenergy 122:211–220. https://doi.org/10.1016/j.biombioe.2019.01.022
5. Harman-Ware AE, Morgan T, Wilson M, Crocker M, Zhang J, Liu K, Stork J, Debolt S (2013) Microalgae as a renewable fuel source: fast pyrolysis of Scenedesmus sp. Renev Energy 60:625–632. https://doi.org/10.1016/j.renene.2013.06.016
6. Derakhshandeh M, Atici T, Un UT (2019) Lipid extraction from microalgae Chlorella and Synechocystis sp. using glass microparticles as disruption enhancer. Energy Environ UK 30(8):1341–1355. https://doi.org/10.1177/0958305X19837463
7. Choi S-A, Lee J-S, Oh Y-K, Jeong M-J, Kim SW, Park J-Y (2014) Lipid extraction from Chlorella vulgaris by molten-salt/ionic-liquid mixtures. Algal Res 3:44–48. https://doi.org/10.1016/j.algal.2013.11.013
8. Brennan L, Owende P (2010) Biofuels from microalgae—a review of technologies for production, processing, and extractions of biofuels and co-products. Renew Sust Energ Rev 14(2):557–577. https://doi.org/10.1016/j.rser.2009.10.009
9. Kandasamy S, Zhang B, He Z, Chen H, Feng H, Wang Q, Wang B, Ashokkumar V, Siva S, Bhuvanendran N (2020) Effect of low-temperature catalytic hydrothermal liquefaction of Spirulina platensis. Energy 190:116236. https://doi.org/10.1016/j.energy.2019.116236
10. Shuping Z, Yulong W, Mingde Y, Chun L, Junmao T (2010) Pyrolysis characteristics and kinetics of the marine microalgae Dunaliella tertiolecta using thermogravimetric analyzer. Bioresour Technol 101(1):359–365. https://doi.org/10.1016/j.biortech.2009.08.020
11. Sotoudehniakarani F, Alayat A, McDonald AG (2019) Characterization and comparison of pyrolysis products from fast pyrolysis of commercial Chlorella vulgaris and cultivated microalgae. J Anal Appl Pyrolysis 139:258–273. https://doi.org/10.1016/j.jaap.2019.02.014
12. Wang K, Brown RC, Homsy S, Martinez L, Sidhu SS (2013) Fast pyrolysis of microalgae remnants in a fluidized bed reactor for bio-oil and biochar production. Bioresour Technol 127:494–499. https://doi.org/10.1016/j.biortech.2012.08.016
13. Anand V, Sunjeev V, Vinu R (2016) Catalytic fast pyrolysis of Arthrospira platensis (spirulina) algae using zeolites. J Anal Appl Pyrolysis 118:298–307
14. Miao X, Wu Q, Yang C (2004) Fast pyrolysis of microalgae to produce renewable fuels. J Anal Appl Pyrolysis 71(2):855–863. https://doi.org/10.1016/j.jaap.2003.11.004
15. Mohan D, Pittman CU, Steele PH (2006) Pyrolysis of wood/biomass for bio-oil: a critical review. Energy Fuel 20(3):848–889
16. Vardon DR, Sharma BK, Blazina GV, Rajagopalan K, Strathmann TJ (2012) Thermochemical conversion of raw and defatted algal biomass via hydrothermal liquefaction and slow pyrolysis. Bioresour Technol 109:178–187. https://doi.org/10.1016/j.biortech.2012.01.008
17. Miao X, Wu Q (2004) High yield bio-oil production from fast pyrolysis by metabolic controlling of Chlorella protothecoides. J Biotechnol 110(1):85–93. https://doi.org/10.1016/j.jbiotec.2004.01.013
18. Yang C, Li R, Qiu Q, Yang H, Zhang Y, Yang B, Wu J, Li B, Wang W, Ding Y (2020) Pyrolytic behaviors of Scenedesmus obliquus over potassium fluoride on alumina. Fuel 263:116724. https://doi.org/10.1016/j.fuel.2019.116724
19. Chen C, Tang J, Guo C, Huang H (2019) Effect of composite additives on microwave-assisted pyrolysis of microalgae. Energy Source PART A:1–11. https://doi.org/10.1080/15567036.2019.1649328
20. Xie Q, Addy M, Liu S, Zhang B, Cheng Y, Wan Y, Li Y, Liu Y, Lin X, Chen P, Ruan R (2015) Fast microwave-assisted catalytic co-pyrolysis of microalgae and scum for bio-oil production. Fuel 160:577–582. https://doi.org/10.1016/j.fuel.2015.08.020
21. Casazza AA, Spennati E, Converti A, Busca G (2020) Production of carbon-based biofuels by pyrolysis of exhausted Arthrospira platensis biomass after protein or lipid recovery. Fuel Process Technol 201:106336
22. Zainan NH, Srivatsa SC, Li F, Bhattacharya S (2018) Quality of bio-oil from catalytic pyrolysis of microalgae Chlorella vulgaris. Fuel 223:12–19. https://doi.org/10.1016/j.fuel.2018.02.166
23. Aysu T, Ola O, Maroto-Valer MM, Sanna A (2017) Effects of titania based catalysts on in-situ pyrolysis of Pavlova microalgae. Fuel Process Technol 166:291–298. https://doi.org/10.1016/j.fuproc.2017.05.001
24. Chan YH, Yusup S, Quitain AT, Tan RR, Sasaki M, Lam HL, Uemura Y (2015) Effect of process parameters on hydrothermal liquefaction of oil palm biomass for bio-oil production and its life cycle assessment. Energy Convers Manag 104:180–188. https://doi.org/10.1016/j.enconman.2015.03.075
25. Grierson S, Strezov V, Bengtsson J (2013) Life cycle assessment of a microalgae biomass cultivation, bio-oil extraction and pyrolysis processing regime. Algal Res 2(3):299–311. https://doi.org/10.1016/j.algal.2013.04.004
26. Peters JF, Banks SW, Bridgwater AV, Dufour J (2017) A kinetic reaction model for biomass pyrolysis processes in Aspen Plus. Appl Energy 188:595–603. https://doi.org/10.1016/j.apenergy.2016.12.030
27. Derakhshandeh M, Atici T, Un UT (2020) Evaluation of wild-type microalgae species biomass as carbon dioxide sink and renewable energy resource. Waste Biomass Valoriz:1–17. https://doi.org/10.1007/s12649-020-00969-8
28. Rippka R, Deruelles J, Waterbury JB, Herdman M, Stanier RY (1979) Generic assignments, strain histories and properties of pure cultures of cyanobacteria. Microbiology 111(1):1–61. https://doi.org/10.1099/00221287-111-1-1
29. Singh G, Patidar S (2018) Microalgae harvesting techniques: a review. J Environ Manag 217:499–508. https://doi.org/10.1016/j.jenvman.2018.04.010

30. Bligh EG, Dyer WJ (1959) A rapid method of total lipid extraction and purification. Can J Biochem Phys 37(8):911–917. https://doi.org/10.1139/o59-099
31. Dubois M, Gilles KA, Hamilton JK, Rebers P, Smith F (1956) Colorimetric method for determination of sugars and related substances. Anal Chem 28(3):350–356. https://doi.org/10.1021/ac60111a017
32. Lourenço SO, Barbarino E, Lavín PL, Lanfer Marquez UM, Aidar E (2004) Distribution of intracellular nitrogen in marine microalgae: calculation of new nitrogen-to-protein conversion factors. Eur J Phycol 39(1):17–32. https://doi.org/10.1080/0967026032000157156
33. Meraz L, Domínguez A, Kornhauser I, Rojas F (2003) A thermochemical concept-based equation to estimate waste combustion enthalpy from elemental composition☆. Fuel 82(12):1499–1507. https://doi.org/10.1016/S0016-2361(03)00075-9
34. Jena U, Das KC, Kastner JR (2011) Effect of operating conditions of thermochemical liquefaction on biocrude production from Spirulina platensis. Bioresour Technol 102(10):6221–6229. https://doi.org/10.1016/j.biortech.2011.02.057
35. Kim KH, Kim J-Y, Cho T-S, Choi JW (2012) Influence of pyrolysis temperature on physicochemical properties of biochar obtained from the fast pyrolysis of pitch pine (Pinus rigida). Bioresour Technol 118:158–162. https://doi.org/10.1016/j.biortech.2012.04.094
36. Ates F, Işıkdağ MA (2008) Evaluation of the role of the pyrolysis temperature in straw biomass samples and characterization of the oils by GC/MS. Energy Fuel 22(3):1936–1943. https://doi.org/10.1021/ef7006276
37. Meesuk S, Cao J-P, Sato K, Ogawa Y, Takarada T (2011) Fast pyrolysis of rice husk in a fluidized bed: effects of the gas atmosphere and catalyst on bio-oil with a relatively low content of oxygen. Energy Fuel 25(9):4113–4121. https://doi.org/10.1021/ef200867q
38. Choi HL, Sudiarto SIA, Renggaman A (2014) Prediction of livestock manure and mixture higher heating value based on fundamental analysis. Fuel 116:772–780. https://doi.org/10.1016/j.fuel.2013.08.064
39. Greenhalf CE, Nowakowski DJ, Harms AB, Titiloye JO, Bridgwater AV (2013) A comparative study of straw, perennial grasses and hardwoods in terms of fast pyrolysis products. Fuel 108:216–230. https://doi.org/10.1016/j.fuel.2013.01.075
40. Grierson S, Strezov V, Shah P (2011) Properties of oil and char derived from slow pyrolysis of Tetraselmis chui. Bioresour Technol 102(17):8232–8240. https://doi.org/10.1016/j.biortech.2011.06.010
41. Zhao C, Kou Y, Lemonidou AA, Li X, Lercher JA (2009) Highly selective catalytic conversion of phenolic bio-oil to alkanes. Angew Chem 121(22):4047–4050. https://doi.org/10.1002/anie.200900404
42. Netscher T (2007) Synthesis of vitamin E. Vitam Horm 76:155–202. https://doi.org/10.1016/S0083-6729(07)76007-7
43. Torri C, Lesci IG, Fabbri D (2009) Analytical study on the production of a hydroxylactone from catalytic pyrolysis of carbohydrates with nanopowder aluminium titanate. J Anal Appl Pyrolysis 84(1):25–30. https://doi.org/10.1016/j.jaap.2008.10.002
44. Dilcio Rocha J, Luengo CA, Snape CE (1999) The scope for generating bio-oils with relatively low oxygen contents via hydropyrolysis. Org Geochem 30(12):1527–1534. https://doi.org/10.1016/S0146-6380(99)00124-2
45. Li J, Yan R, Xiao B, Wang X, Yang H (2007) Influence of temperature on the formation of oil from pyrolyzing palm oil wastes in a fixed bed reactor. Energy Fuel 21(4):2398–2407. https://doi.org/10.1021/ef060548c
46. Onay O (2007) Influence of pyrolysis temperature and heating rate on the production of bio-oil and char from safflower seed by pyrolysis, using a well-swept fixed-bed reactor. Fuel Process Technol 88(5):523–531. https://doi.org/10.1016/j.fuproc.2007.01.001
47. Guo F, Wang X, Yang X (2017) Potential pyrolysis pathway assessment for microalgae-based aviation fuel based on energy conversion efficiency and life cycle. Energy Convers Manag 132:272–280. https://doi.org/10.1016/j.enconman.2016.11.020
48. Jena U, Das KC, Kastner JR (2012) Comparison of the effects of Na2CO3, Ca3(PO4)2, and NiO catalysts on the thermochemical liquefaction of microalga Spirulina platensis. Appl Energy 98:368–375. https://doi.org/10.1016/j.apenergy.2012.03.056
49. Saudi Aramco Anual Review 2016, The many layers of oppurtunity (2016). Aramco Company